Proc. Natl. Acad. Sci. USA
Vol. 95, pp. 13800–13805, November 1998
Genetics

Rump white inversion in the mouse disrupts dipeptidyl aminopeptidase-like protein 6 and causes dysregulation of *Kit* expression

R. Barry Hough*, Andreas Lengeling*, Vahe Bedian†, Cecilia Lo‡, and Maja Bućan*†§

*Center for Neurobiology and Behavior of the Department of Psychiatry, and Departments of †Genetics and ‡Biology, University of Pennsylvania, Philadelphia, PA 19104

Edited by Shirley M. Tilghman, Princeton University, Princeton, NJ, and approved September 1, 1998 (received for review August 5, 1998)

ABSTRACT **The mouse *rump white* (*Rw*) mutation causes a pigmentation defect in heterozygotes and embryonic lethality in homozygotes. At embryonic day (E) 7.5, *Rw*/*Rw* embryos are retarded in growth, fail to complete neurulation and die around E 9.5. The *Rw* mutation is associated with a chromosomal inversion spanning 30 cM of the proximal portion of mouse chromosome 5. The *Rw* embryonic lethality is complemented by the W^{19H} deletion, which spans the distal boundary of the *Rw* inversion, suggesting that the *Rw* lethality is not caused by the disruption of a gene at the distal end of the inversion. Here, we report the molecular characterization of sequences disrupted by both inversion breakpoints. These studies indicate that the distal breakpoint of the inversion is associated with ectopic *Kit* expression and therefore may be responsible for the dominant pigmentation defect in *Rw*/+ mice; whereas the recessive lethality of *Rw* is probably due to the disruption of the gene encoding dipeptidyl aminopeptidase-like protein 6, *Dpp6* [Wada, K., Yokotani, N., Hunter, C., Doi, K., Wenthold, R. J. & Shimasaki, S. (1992) *Proc. Natl. Acad. Sci. USA* 89, 197–201] located at the proximal inversion breakpoint.**

Classical genetic studies of the mouse have involved extensive analyses of coat color mutations. Using tester strains that harbor coat color mutations, large scale mutagenesis screens expanded the collection of alleles at loci, such as agouti, brown, albino, *dilute*, *pink-eyed dilution*, *short ear*, *piebald-spotting*, and others (1). Molecular isolation of genes disrupted in these mutations and characterization of their allelic series revealed new genetic pathways that control developmental processes and basic aspects of cell signaling (2, 3).

A cluster of coat color mutations in the central portion of mouse chromosome 5 includes *white spotting* (*W*), *patch* (*Ph*), and *rump white* (*Rw*) (4). The various alleles of *W* disrupt the structure or expression of *Kit* receptor tyrosine kinase (5–9). The role of *Kit* in the intracellular signal transduction pathways in many distinct cell types is reflected by the pleiotropic affect of *W* on primordial germ cells, hematopoietic cells, melanocytes, and interstitial cells of Cajal in the small intestine, (9, 10). The *Ph* mutation is associated with a deletion encompassing another receptor tyrosine kinase gene, *Pdgfra* (11–14). Homozygous *Ph*/*Ph* mice die between embryonic day (E) 9 and E 16 and show severe morphological anomalies (11, 15), with some but not all anomalies observed in embryos with the targeted null-mutation for PDGFαR (16). However, the pigmentation defect apparent in *Ph*/+ mice cannot be attributed to haploinsufficiency of PDGFRα (16). Expression analysis combined with physical mapping of the *Ph* deletion and regulatory alleles of *W* (W^{bd} and W^{sh}) (6, 17, 18), suggested the alteration of long range cis-regulatory elements, which cause ectopic expression of *Kit* in the dermatome of the somites at E 10.5 and E 11.5. Misregulation of *Kit*, primarily its ectopic expression in neural crest-derived melanoblasts, leads to the abnormal pigment patterns in these mutations, possibly by altering melanocyte dispersal and survival (19, 20).

The least characterized mutation in this cluster, *Rw*, is associated with depigmentation of the sacrolumbar region in heterozygotes, whereas homozygotes die *in utero* during early postimplantation development (4). *Rw*/*Rw* embryos form three germ layers but arrest after E 7.5 at the end of gastrulation (21). Whereas suppressed recombination between the *Rw* and the wild-type chromosomes suggested a large chromosomal rearrangement on the *Rw* chromosome, physical mapping by fluorescense *in situ* hybridization unequivocally revealed an inversion, named In(5)6H, spanning 30 cM in the proximal third of mouse chromosome 5 (ref. 22 and this publication). The proximal breakpoint of the *Rw* inversion lies centromeric to the *En2* locus, whereas the distal breakpoint maps to the region between the *Kit* and *Pdgfra* genes in the central portion of the chromosome (14, 22). These studies suggested that the dominant pigmentation defect in *Rw* also could be attributed to the long range effect on *Kit* expression in melanocyte precursors (14, 19). The *Rw* embryonic lethality is complemented by the W^{19H} deletion, which spans the distal boundary of the *Rw* inversion, suggesting that the *Rw* lethality is not caused by the disruption of a gene at the distal end of the inversion (14, 23). Therefore, assuming a simple chromosomal rearrangement, the disrupted gene causing the lethality may map to the proximal inversion breakpoint.

To gain further insight into the molecular basis underlying the developmental defects associated with the *Rw* mutation, we undertook the molecular cloning and characterization of the *Rw* inversion breakpoints and sequences surrounding both ends of the *Rw* inversion. Here, we report that the loss or rearrangement of sequences flanking the distal breakpoint causes misregulation of *Kit*, expressed from the *Rw* chromosome. Our analysis found that the proximal breakpoint disrupts the previously described *Dpp6* gene, encoding dipeptidyl peptidase-like protein 6 (24). The embryonic form of *Dpp6* is expressed in wild-type embryos at early post-implantation stages, suggesting that the disruption of *Dpp6* is the underlying cause of the *Rw*/*Rw* lethality. This finding suggests the possibility that DPP6 may have a novel function in embryonic development.

MATERIALS AND METHODS

Mice. Inbred strains of mice (C57BL/6J and C3H/HeJ) and the W^{19H} mutation were obtained from the Jackson Laboratory

The publication costs of this article were defrayed in part by page charge payment. This article must therefore be hereby marked "*advertisement*" in accordance with 18 U.S.C. §1734 solely to indicate this fact.

This paper was submitted directly (Track II) to the *Proceedings* office.
Abbreviations: E, embryonic day; PFGE, pulsed field gel electrophoresis analysis; *Rw*, *Rump white*; Dpp6, dipeptidyl aminopeptidase-like protein 6.

Data deposition: The sequences reported in this paper have been deposited in the GenBank database [accession nos. AF092505 (*Kit-pdgfra* intergenic region), AF092506 (brain *Dpp6* cDNA), AF092507 (embryo *Dpp6* cDNA), and AF095717 (proximal breakpoint of *Rw* inversion)].

§To whom reprint requests should be addressed. e-mail: bucan@pobox.upenn.edu.

(Bar Harbor, ME). *Rw* mice were provided by Colin Beechey and Bruce Cattanach, Medical Research Council, Radiobiology Unit, Harwell, UK.

Pulsed-Field Gel Electrophoresis Analysis. Methods for pulsed-field gel electrophoresis, including DNA preparation of agarose blocks and restriction analysis have been described previously (25).

Generation and Screening of Cosmid Libraries. The genomic cosmid library of *Rw*/+ DNA and subgenomic cosmid library of YAC B20.S3.RA.C6 in SuperCos 1 vector were constructed according to manufacturer's instructions (Stratagene). Colonies were plated and screened according to published protocols (25).

cDNA Library Screening. A E 8.5 mouse cDNA library, cloned in λZAP II (Stratagene) and provided by P. Labosky and K. Mahon, was screened by using the radiolabeled 3-kb *Dpp6*–*Eco*RI fragment.

Sequencing and Sequence Analysis. Automated dideoxy terminator cycle sequencing was carried out on cosmid and plasmid DNA by using Dye Terminator sequencing chemistry with *Taq* FS polymerase from Applied Biosystems. Reaction products were purified by G50 spin columns and analyzed on Applied BioSystems 373A and 377 automated sequencers. Sequence files were edited and assembled into contigs by using the SEQUENCHER software (GeneCodes, Ann Arbor, MI). For coding sequence identification, genomic sequences were systemically analyzed with BLASTN and BLASTX alogorithms against public databases. Exon predictions were performed with GRAIL1 and GRAIL2, GENE FINDER, and GENIE programs.

Southern Blot Hybridization. DNA separated by pulsed field gel electrophoresis analysis (PFGE) or by conventional electrophoresis was transferred to Hybond N+ (Amersham) membrane by capillary blotting in denaturation buffer (25, 26). Filters were UV crosslinked (autocrosslink set up on Stratalinker; Stratagene) and hybridized at 65°C in hybridization buffer. Filters were washed in 0.1× SSC; 0.1% SDS at 65°C.

RNA Analysis. For Northern blot hybridization, tissue was collected from C57BL/6J and *Rw*/+ mice. The extraction of total RNA was done by using standard protocols (27). Fifteen micrograms of total RNA was separated in a 1% denaturing formaldehyde gel, transferred to Hybond N (Amersham) membrane, and UV crosslinked (autocrosslink set up on Stratalinker; Stratagene). Hybridization was performed at 65°C in hybridization buffer (25). Filters were washed in 0.1× SSC; 0.1% SDS at 65°C.

***In Situ* Hybridization.** For *in situ* hybridization, embryos were fixed in modified Carnoy's fixative and embedded in paraffin. Embryos were sectioned at 6 μM, and slides were hybridized and washed as described previously (28). Slides were then dipped into XL emmulsion (Eastman Kodak) and developed after several weeks.

RESULTS

Isolation of Sequences Disrupted by the Distal Breakpoint of the *Rw* Inversion. Analysis of the *Rw* chromosome by fluorescent *in situ* hybridization and PFGE placed the distal breakpoint of the *Rw* inversion between *Pdgfra* and *Kit* (14) (Fig. 1*A*). A YAC clone spanning the region around the distal breakpoint was isolated (29), and a subgenomic cosmid library was used to perform a chromosome walk between *D5Buc3* and *Kit* (Fig. 1*A*). To refine the position of the breakpoint region, unique hybridization probes from the cosmid walk were used in PFGE analysis of *Rw*/+ and +/+ (C57BL/6J and C3H/HeJ) DNA (Fig. 1 *B* and *C*). A *Pdgfra* probe and several probes isolated from cosmids cRBH1 through cRBH5 displayed distinct hybridization profiles in +/+ and *Rw*/+ DNA. For example, *Pdgfra* and probe *D5Buc4*, detected a 440-kb *BssH*II DNA fragment on the wild-type chromosome but also hybridized to a 1,000-kb rearranged *BssH*II DNA fragment in *Rw*/+ (Fig. 1*B*). However, the probe *D5Buc5*, located on the adjacent cosmid cRBH5, hybridized to a *Rw*-specific fragment of a different size (>1,500 kb). Other probes located distal to cRBH5 also detected this *Rw*-specific PFGE fragment. These findings show that *D5Buc5*, located by PFGE analysis 160–220 kb proximal to *Kit*, maps outside the *Rw* inversion and that cRBH5 spans the distal inversion breakpoint (Fig. 1).

Based on PFGE analysis, the *D5Buc3-Kit* region also should contain the distal breakpoint for the *Ph* deletion (14). The *Pdgfra* locus, *D5Buc3*, and several loci defined by probes from the cosmids cRBH1–4 (including *D5Buc4*) were found to be deleted in the *Ph* mutation (Fig. 1*D*; refs. 12 and 14 and data not shown). However, *D5Buc5* detected the distal breakpoint of the *Rw* inversion and also detected rearranged fragments in PFGE analysis of *Ph*/+ DNA (Fig. 1 *A* and *C*). Moreover, hybridization of probes *D5Buc4* and *D5Buc5* to Southern blots containing *Ph*/+ DNA showed that the same 3.9-kb *Bam*HI DNA fragment disrupted by the distal breakpoint of the *Rw* inversion also flanks the distal breakpoint of the *Ph* deletion (Fig. 1 and data not shown). We performed nucleotide sequence analysis of 10 kb of wild-type DNA surrounding the disrupted 3.9-kb *Bam*HI fragment. Analysis of the sequenced region did not reveal homology to any known genes or expressed sequence tags (in GenBank and Swissprot databases), or potential coding sequences, as determined by GRAIL 2 and GENE FINDER. Moreover, cRBH5 did not detect transcripts when hybridized to multiple tissue Northern blots (data not shown), and therefore it is unlikely that the distal breakpoints of *Rw* and *Ph* rearrangements disrupt coding sequences of a structural gene. However, several inverted repeat sequences surrounding the closely located breakpoints may represent elements that facilitated chromosome breakage in these two independently isolated mutations.

The Long-Range Effect of the *Rw* Inversion on *Kit* Expression. Discovery that the distal breakpoint of the *Rw* inversion occurs in the same genomic region as the breakpoints of the *Ph* deletion and several regulatory alleles of *W* (W^{bd}, W^{sh}, and W^{57}) (6, 17, 18, 26) suggested that the pigmentation defect associated with the *Rw* mutation might be due to long-range effects on *Kit* expression. In fact, the examination of *Kit* expression by *in situ* hybridization analysis revealed that *Kit* is ectopically expressed from the *Rw* chromosome (Fig. 2).

In situ expression analysis was carried out using *Rw*+/+W^{19H} compound heterozygous embryos because deletion of *Kit* on the W^{19H} chromosome allows for the examination of *Kit* expression specifically from the *Rw* chromosome. These studies showed that *Kit* is ectopically expressed in the dorsal neural tube in *Rw*+/+W^{19H} embryos (Fig. 2 *I* and *J*); interestingly, a similar expression pattern is seen in *Ph*/+ embryos (17, 19). In addition, *Kit* was observed to be ectopically expressed in the *Rw*+/+W^{19H} dermatome and heart (Fig. 2*G–J*), a pattern that is similar to that seen with W^{bd} and W^{sh} (6, 18). In contrast, we observed little or no *Kit* expression in the surface ectoderm and otic vesicle (Fig. 2 *E*, *F*, *I* and *J*), suggesting that melanoblasts may be reduced in numbers. This possibility is supported by the finding of reduced expression of an early melanoblast marker, tyrosinase-related protein-2 (TRP2) in the otic vesicle (ref. 20 and data not shown) and the fact that adult *Rw*+/+W^{19H} mice are almost completely depigmented. Overall, our data indicate that the *Rw* inversion breakpoint located 160–220 kb proximal to *Kit* has tissue-specific effects on *Kit* expression during embryogenesis and may be responsible for the dominant pigmentation defect associated with the *Rw* mutation.

***Dpp6* Is Disrupted by the Proximal Breakpoint of the *Rw* Inversion.** The identification of genomic sequences at the distal breakpoint of the *Rw* inversion provided the means for isolating sequences juxtaposed to this region on the inverted chromosome. To clone sequences around the proximal breakpoint, a cosmid library of *Rw*/+ DNA was screened with the *D5Buc4* probe (Fig. 1). Restriction analysis showed that an isolated cosmid, cAB1, contains sequences that span the proximal inversion breakpoint. Nucleotide sequence analysis of 29 kb flanking the breakpoint

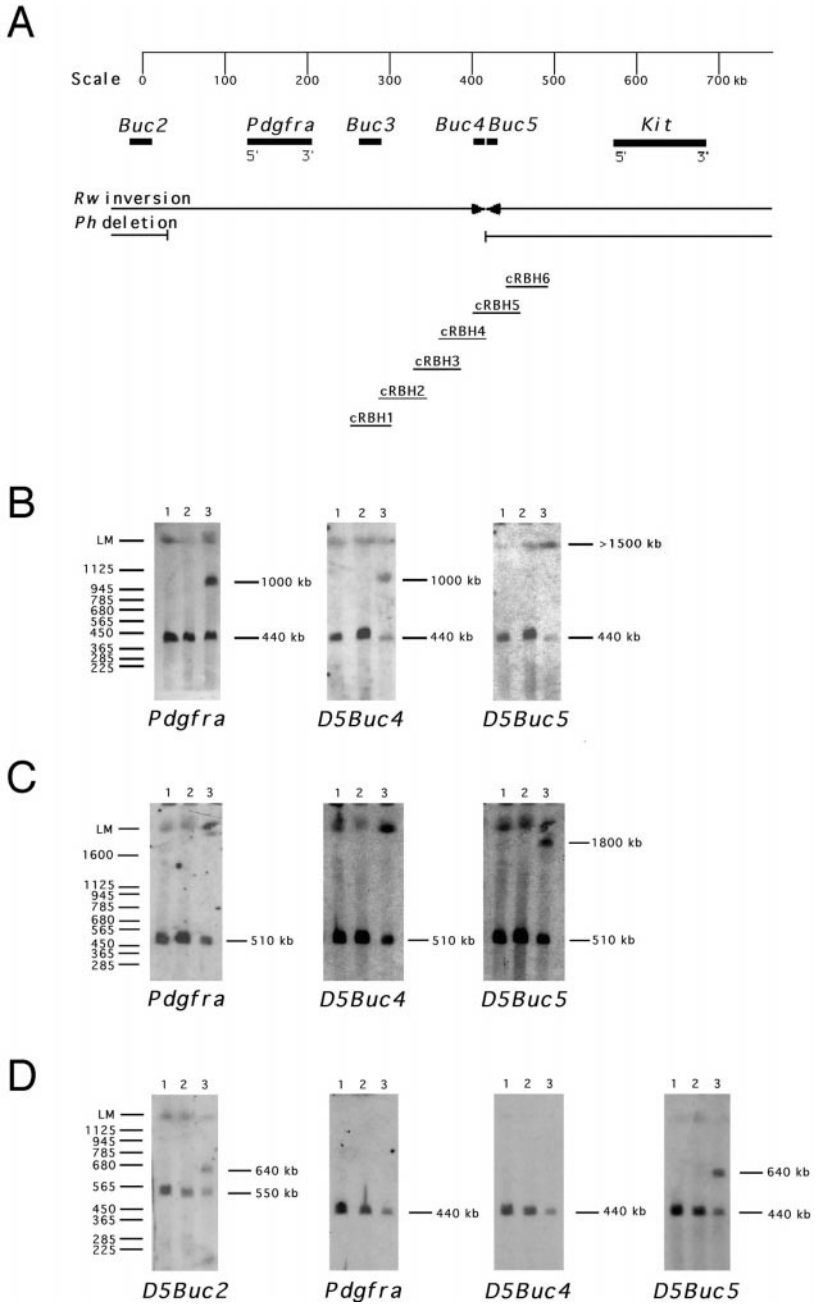

FIG. 1. PFGE analysis of the chromosomal rearrangements associated with the *Rw* and *Ph* mutations. (*A*) Map positions of the loci *Pdgfra*, *Kit*, *D5Buc2*, *D5Buc3*, *D5Buc4*, and *D5Buc5* relative to the chromosomal rearrangements associated with *Ph* and *Rw*. The probes *D5Buc2* and *D5Buc3* are described previously (14, 26), and the probes *D5Buc4* and *D5Buc5* are unique probes from cosmids cRBH4 and cRBH5, respectively, as described in the text. (*B*) PFGE analysis of the *Rw* mutation: C57BL/6J (lane 1), C3H/He (lane 2), and *Rw*/+ (lane 3) DNA digested with *Bss*HII hybridized with *Pdgfra*, *D5Buc4*, and *D5Buc5*. (*C*) PFGE analysis of the *Rw* mutation: C57BL/6J (lane 1), C3H/He (lane 2), and *Rw*/+ (lane 3) DNA digested with *Not*I hybridized with *Pdgfra*, *D5Buc4*, and *D5Buc5*. (*D*) PFGE analysis of the *Ph* mutation. C57BL/6J (lane 1), C3H/He (lane 2), and *Ph*/+ (lane 3) DNA digested with *Bss*HII hybridized with *Pdgfra*, *D5Buc2*, *D5Buc4*, and *D5Buc5*. The sizes (in kb) of DNA fragments are shown on the right.

identified four exons corresponding to the gene encoding dipeptidyl aminopeptidase-like protein 6, *Dpp6* (24, 30) (Fig. 3*B*). Chromosomal localization of the *Dpp6* gene to the subcentromeric portion of mouse chromosome 5 (31) further confirmed that the isolated sequences span the inversion breakpoint. The DPP6 protein is composed of a short N-terminal cytoplasmic domain, a transmembrane domain, and a long C-terminal extracellular domain (Fig. 3*B*) and has been shown to lack peptidase activity (24, 32). In the rat, two *Dpp6* transcripts, 4.4 and 3.6 kb in length, (*DPPX-LV* and *DPPX-SV*), are expressed in the central nervous system whereas a shorter form has a more widespread expression (24, 30). We isolated a mouse cDNA by screening a E 8.5 cDNA library. This embryonic cDNA differs from the reported adult brain isoforms in the first 20 N-terminal amino acids of the hypothetical intracellular domain (Fig. 3*B* and L. deLecea and G. Sutcliffe, unpublished data).

Genomic analysis of the *Dpp6* gene on the *Rw* chromosome places the inversion breakpoint in the coding region between codons corresponding to amino acids 495 and 496 of the predicted protein. These data predict that the inverted chromosome would encode a protein that is missing a significant fraction of the C-terminal region (Fig. 3*B*). Northern blot analysis confirmed the expression of *Dpp6* gene in the adult brain (30); however, truncated transcripts predicted by the

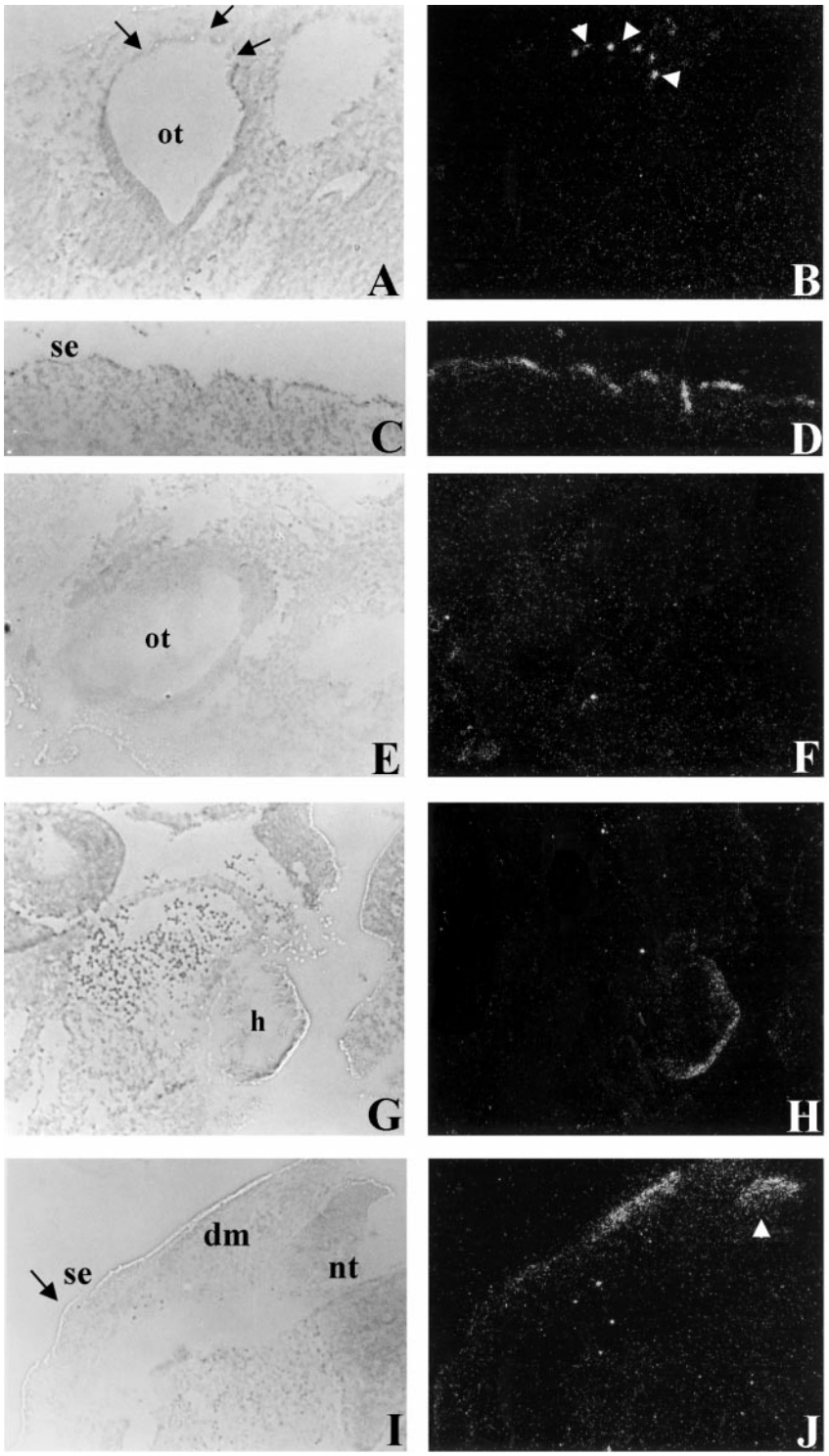

FIG. 2. *In situ* hybridization of *Kit* to wild-type and $Rw+/+W^{19H}$ embryos. The expression of *Kit* in the otic vesicle (ot) in wild-type (*A* and *B*) and the absence of *Kit* expression in $Rw+/+W^{19H}$ (*E* and *F*). Ectopic expression of *Kit* is seen in $Rw+/+W^{19H}$ embryos in the heart (h) (*G* and *H*). The expression of *Kit* in a parasagital section of the surface ectoderm (se) in a wild-type E 10.5 embryo (*C* and *D*) and the absence of or reduced expression in transverse sections of surface ectoderm (se, see region denoted by black arrow) from a $Rw+/+W^{19H}$ embryo (*I* and *J*). Note that the plane of section in the wild-type (*C*) is equivalent to the region denoted by the black arrows in the $Rw+/+W^{19H}$ section (*I*). Ectopic expression is seen in $Rw+/+W^{19H}$ embryos in the dermatome (dm) (*I* and *J*) and the dorsal region of the neural tube (nt) (see white arrow head in *J*).

genomic rearrangement were not detected in *Rw* mutant RNA (Fig. 4*A*). A comparison of steady–state levels of expression of the two *Dpp6* transcripts (3.6 and 4.4 kb) in brains of adult *Rw*/+ and +/+ mice with the level of expression of β actin in the same tissue, shows that *Dpp6* is either not expressed from the *Rw* chromosome or that its truncated message is unstable (Fig. 4*A*). To investigate whether the disruption of *Dpp6* may cause the embryonic lethality of *Rw*/*Rw* embryos, we examined the expression of *Dpp6* during embryogenesis by Northern blot analysis (Fig. 4*B*). The two adult mRNA forms of *Dpp6* were detected at E 11, E 15, and E 17, whereas at E 7 a transcript of intermediate size, corresponding to the length of the embryonic cDNA clone (3,842 bp), was found to be expressed at a lower level.

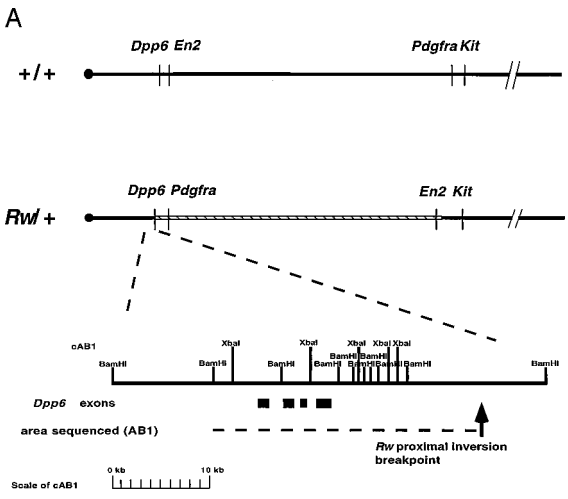

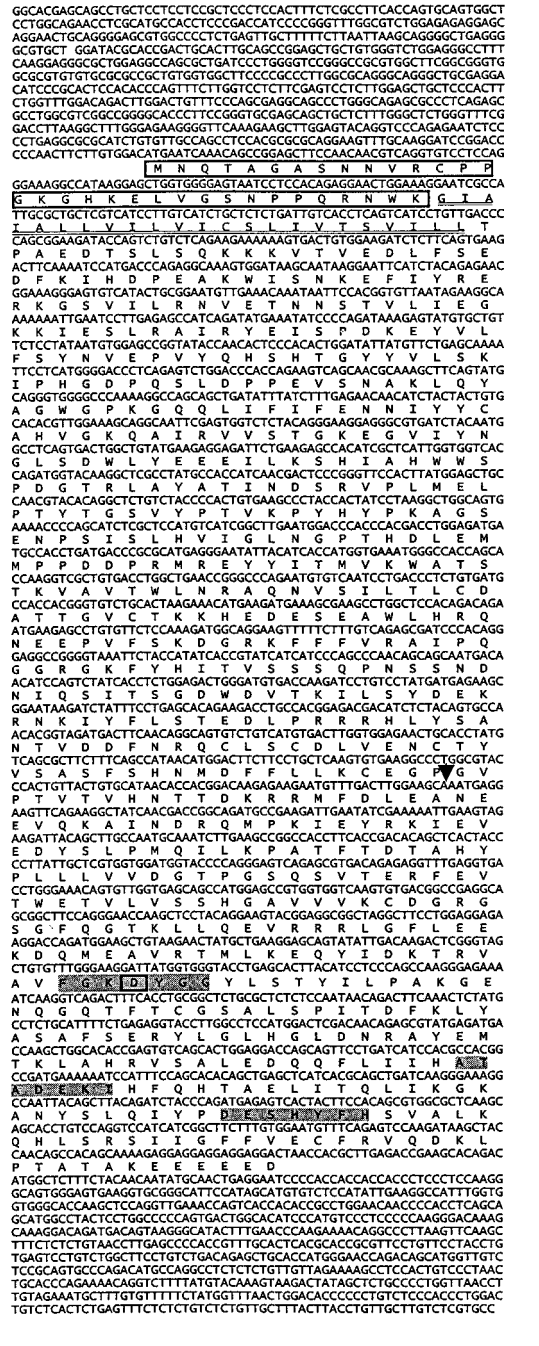

DISCUSSION

This study describes the molecular characterization of the *Rw* inversion breakpoints; the distal breakpoint, located 160–220 kb proximal to *Kit*, probably does not disrupt any transcribed sequences, although it causes ectopic expression of the *Kit* gene in dermatome, neural tube, and heart at E 10.5. The proximal breakpoint disrupts the gene encoding the dipeptidyl aminopeptidase-like protein 6. This gene of unknown function is expressed in wild-type embryos at an early postimplantation stage when *Rw*/*Rw* embryos die and therefore represents a candidate gene for the *Rw* lethality factor.

The observed overexpression of *Kit* in $Rw+/+W^{19H}$ embryos and in the previously described W^{sh} and W^{bd} mutants, supports the hypothesis of Duttlinger *et al.* (6, 18) that sequestration of soluble Steel factor, the KIT ligand, by ectopic *Kit* expression in the dermatome decreases Steel availability to melanoblasts, thereby causing the pigmentation defect seen in adults (6, 17, 19, 33). However, the observation of altered *Kit* expression in $Rw+/+W^{19H}$ embryos should be interpreted with caution because the analysis was conducted on compound heterozygote embryos, containing only one *Kit* allele. Therefore, the observed pattern of *Kit* expression may be due to the synergistic interaction between *Rw* and W^{19H}. The pigmentation defect in the sacrolumbar region in *Rw*/+ mice is distinct and different from the "sash-like" depigmentation in *Ph*, W^{sh}, W^{bd}, and W^{57}. Given that different chromosomal rearrangements associated with *Ph*, *Rw*, and *W* alleles display similar or overlapping patterns of *Kit* expression, it is likely that the loss or juxtaposition of tissue-specific cis-regulatory elements, rather than position-effects on the chromatin structure (34), underlie such long-range effects. However, our data do not permit us to correlate the molecular nature or position of these disrupted sequences with the range of phenotypic anomalies observed in different alleles. Physical mapping has placed chromosomal rearrangements associated with the *Ph* and *Rw* mutations and regulatory alleles of *W* at different positions in the *Pdgfra-Kit* intergenic region; with the breakpoints of the *Ph* deletion and the *Rw* inversion further proximal of the 5′ region of *Kit* than the breakpoints of the W^{sh} and W^{bd} inversions and W^{57} deletion (6, 17, 18, 26).

A central question is whether the disruption of the *Dpp6* gene leads to the developmental arrest and embryonic lethality of *Rw*/*Rw* embryos. The biological function of this cell-surface peptidase-like protein is still unresolved. DPP6 protein probably does not possess endopeptidase activity because of an amino acid substitution in the catalytic domain (24, 32). The presence of at least three different forms of the intracellular domain of *Dpp6* at different stages of embryonic development and in adult tissues implies that these three DPP6 isoforms may have different

FIG. 3. Genomic structure of the proximal *Rw* inversion breakpoints. (*A*) Wild-type and *Rw* chromosomal maps give the approximate map positions of genes based on previous studies (14, 22, 31). The *Rw* inversion is represented by a cross-hatched box. Cosmid cAB1 was isolated by screening a genomic library of *Rw*/+ DNA with a unique probe from cRBH5 (*D5Buc4*) as described in the text. Chromosomal distances are not represented on scale. The restriction map of cAB1 is shown. Dashed lines indicate the sequenced region. Solid lines below cAB1 give the approximate positions of *Dpp6* exons found by sequencing and GRAIL2 analysis. Arrow shows the positions of the inversion breakpoint. (*B*) Sequence analysis of the embryonic *Dpp6* cDNA (GenBank accession no. AF092507). Shown are the cDNA sequence and the deduced amino acid sequence. The putative intracellular domain is boxed and the transmembrane domain double underlined. The first 20 amino acids are unique in the embryonic DPP6 isoform. The conserved residues, which form the putative catalytic site in nonclassical serine peptidases, are gray shaded, and the aspartic residue, which is replaced by a serine residue shown to be essential for peptidase activity in DPP4, is boxed (32). The location of the proximal *Rw* inversion breakpoint, which eliminates the C-terminal portion of DPP6, is indicated by an arrowhead.

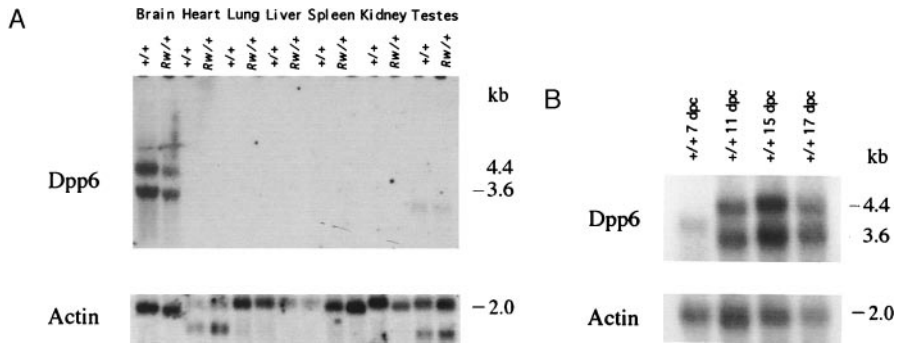

FIG. 4. Expression analysis of *Dpp6* on the *Rw* and +/+ chromosome. (*A*) Northern blot analysis of *Dpp6* in +/+ and *Rw*/+ mice. The *Dpp6* cDNA probe detects 4.4 kb and 3.6 kb transcripts in the brain of +/+ and of *Rw*/+. A transcript of 3.4 kb also was detected in the testes of +/+ and of *Rw*/+. Total RNA was isolated from adult tissue. RNA loading was assessed by hybridization with β actin and a phosphorimager was used to quantitate and compare levels of expression in +/+ and *Rw*/+ RNA samples. (*B*) Analysis of *Dpp6* expression in embryonic RNA samples. The probe for *Dpp6* detects a 4.4 kb and a 3.6 kb transcripts in 11- to 17-day mouse embryos. A transcript of 3.9 kb was detected in 7-day mouse embryos. The Northern filter (CLONTECH) contains 2 μg of polyadenlyated RNA from E 7, E 11, E 15, and E 17 mouse embryos. RNA loading was assessed by hybridization with β actin.

functions. *Dpp6* is highly expressed in the hippocampus, thalamus, hypothalamus, and striatum and may be involved in neuronal plasticity (30). However, how this predicted role might relate to its role in early postimplantation development remains to be determined. To confirm that the disruption of *Dpp6* causes embryonic lethality in *Rw*, it will be necessary to show that this mutation fails to complement a second loss-of-function mutation in *Dpp6* or that *Rw*/*Rw* lethality can be rescued by a *Dpp6* transgene. Such studies are currently in progress. However, complementation between *Rw* and loss-of-function allele of *Dpp6* would indicate that an independent mutation within the inverted region—a region of suppressed recombination—is responsible for the lethality. The use of the *Rw* chromosome as a balancer in an ongoing region-specific screen for *N*-ethyl-*N*-nitrosourea-induced mutations in the proximal portion of mouse chromosome 5 (35), may facilitate molecular characterization of the gene(s) causing the lethality associated with this mutation.

We thank L. de Lecea and G. Suttcliffe for the *Dpp6* probe, B. Pavan, K. Steel, and I. Jackson for tyrosinase-related protein-2 (TRP2), K. Steel and A. Bernstein for *Kit* probes, P. Labosky for the E 8.5 mouse cDNA library, A. Alavizadeh and M. Cohen for help with the expression analysis, M. Santoro of the DNA Sequencing Facility for technical assistance in sequencing and primer walking, and S. Poethig, L. Stubbs, and J. Schimenti for their comments on the manuscript. These studies were supported by National Institutes of Health Grants HD 28410 (to M.B.) and HD 36457 (to C.L.) and National Science Foundation Grant IBN31544 (to C.L.).

1. Russell, W. L. (1951) *Cold Spring Harbor Symp. Quant. Biol.* **16,** 327–336.
2. Jackson, I. J. (1994) *Annu. Rev. Genet.* **28,** 189–217.
3. Barsh, G. S. (1996) *Trends Genet.* **12,** 299–305.
4. Searle, A. G. & Truslove, G. M. (1970) *Genet. Res.* **15,** 227–235.
5. Chabot, B., Stephenson, D. A., Chapman, V. M., Besmer, P. & Bernstein, A. (1988) *Nature (London)* **335,** 88–89.
6. Duttlinger, R., Manova, K., Chu, T. Y., Gyssler, C., Zelenetz, A. D., Bachvarova, R. F. & Besmer, P. (1993) *Development (Cambridge)* **118,** 705–717.
7. Geissler, E. N., Ryan, M. A. & Housman, D. E. (1988) *Cell* **55,** 185–192.
8. Nocka, K., Tan, J. C., Chiu, E., Chu, T. Y., Ray, P., Traktman, P. & Besmer, P. (1990) *EMBO J.* **9,** 1805–1813.
9. Reith, A. D., Rottapel, R., Giddens, E., Brady, C., Forrester, L. & Bernstein, A. (1990) *Genes Dev.* **4,** 390–400.
10. Huizinga, J. D., Thuneberg, L., Kluppel, M., Malysz, J., Mikkelsen, H. B. & Bernstein, A. (1995) *Nature (London)* **373,** 347–349.
11. Gruneberg, H. & Truslove, G. M. (1960) *Genet. Res.* **1,** 69–90.
12. Stephenson, D. A., Mercola, M., Anderson, E., Wang, C., Stiles, C. D., Bowen-Pope, D. F. & Chapman, V. M. (1991) *Proc. Natl. Acad. Sci. USA* **88,** 6–10.
13. Smith, E. A., Seldin, M. F., Martinez, L., Watson, M. L., Choudhury, G. G., Lalley, P. A., Pierce, J., Aaronson, S., Barker, J., Naylor, S. L., *et al.* (1991) *Proc. Natl. Acad. Sci. USA* **88,** 4811–4815.
14. Nagle, D. L., Martin-DeLeon, P., Hough, R. B. & Bucan, M. (1994) *Proc. Natl. Acad. Sci. USA* **91,** 7237–7241.
15. Schatteman, G. C., Morrison-Graham, K., van Koppen, A., Weston, J. A. & Bowen-Pope, D. F. (1992) *Development (Cambridge)* **115,** 123–131.
16. Soriano, P. (1997) *Development (Cambridge)* **124,** 2691–2700.
17. Duttlinger, R., Manova, K., Berrozpe, G., Chu, T.-Y., DeLeon, V., Timokhina, I., Chaganti, R. S. K., Zelenetz, A. D., Bachvarova, R. F. & Besmer, P. (1995) *Proc. Natl. Acad. Sci. USA* **92,** 3754–3758.
18. Kluppel, M., Nagle, D. L., Bucan, M. & Bernstein, A. (1997) *Development (Cambridge)* **124,** 65–77.
19. Wehrle-Haller, B., Morrison-Graham, K. & Weston, J. A. (1996) *Dev. Biol.* **177,** 463–474.
20. Cable, J., Jackson, I. J. & Steel, K. P. (1995) *Mech. Dev.* **50,** 139–150.
21. Bucan, M., Nagle, D. L., Hough, R. B., Chapman, V. M. & Lo, C. W. (1995) *Dev. Biol.* **168,** 307–318.
22. Stephenson, D. A., Lee, K.-H., Nagle, D. L., Yen, C.-H., Morrow, A., Miller, D., Chapman, V. M. & Bucan, M. (1994) *Mamm. Genome* **5,** 342–348.
23. Lyon, M. F., Glenister, P. H., Loutit, J. F., Evans, E. P. & Peters, J. (1984) *Genet. Res.* **44,** 161–168.
24. Wada, K., Yokotani, N., Hunter, C., Doi, K., Wenthold, R. J. & Shimasaki, S. (1992) *Proc. Natl. Acad. Sci. USA* **89,** 197–201.
25. Herrmann, B. G., Barlow, D. P. & Lehrach, H. (1987) *Cell* **48,** 813–825.
26. Nagle, D. L., Kozak, C. A., Mano, H., Chapman, V. M. & Bucan, M. (1995) *Hum. Mol. Genet.* **4,** 2073–2079.
27. Sambrook, J., Fritsch, E. F. & Maniatis, T. (1989) *Molecular Cloning: A Laboratory Manual* (Cold Spring Harbor Lab. Press, Plainview, NY).
28. Ruangvoravat, C. P. & Lo, C. W. (1992) *Dev. Dyn.* **194,** 261–281.
29. Brunkow, M. E., Nagle, D. L., Bernstein, A. & Bucan, M. (1995) *Genomics* **25,** 421–432.
30. de Lecea, L., Soriano, E., Criado, J. R., Steffensen, S. C., Henriksen, S. J. & Sutcliffe, J. G. (1994) *Mol. Brain Res.* **25,** 286–296.
31. Wada, K., Zimmerman, K. L., Adamson, M. C., Yokotani, N., Wenthold, R. J. & Kozak, C. A. (1993) *Mamm. Genome* **4,** 234–237.
32. Yokotani, N., Doi, K., Wenthold, R. J. & Wada, K. (1993) *Hum. Mol. Genet.* **2,** 1037–1039.
33. Wehrle-Haller, B. & Weston, J. A. (1995) *Development (Cambridge)* **121,** 731–742.
34. Hendrich, B. D. & Willard, H. F. (1995) *Hum. Mol. Genet.* **4,** 1765–1777.
35. Schimenti, J. & Bucan, M. (1998) *Genome Res.* **8,** 698–710.